Effect of deleting four *Toxoplasma gondii* calcium binding EGF domain-containing proteins on parasite replication and virulence

Xin-Cheng Wang[1] · **Ting-Ting Li**[1,2] · **Hany M. Elsheikha**[3] · **Xiao-Nan Zheng**[4] · **Dan-Yu Zhao**[1] · **Jin-Lei Wang**[1,2] · **Meng Wang**[1,2] · **Xing-Quan Zhu**[1,4,5]

(✉) Xing-Quan Zhu
xingquanzhu1@hotmail.com
(✉) Meng Wang
wangmeng02@caas.cn

[1] State Key Laboratory of Veterinary Etiological Biology, Key Laboratory of Veterinary Parasitology of Gansu Province, Lanzhou Veterinary Research Institute, Chinese Academy of Agricultural Sciences, Lanzhou, Gansu Province 730046, PR China
[2] Institute of Urban Agriculture, Chinese Academy of Agricultural Sciences, Chengdu, Sichuan Province 610213, PR China
[3] Faculty of Medicine and Health Sciences, School of Veterinary Medicine and Science, University of Nottingham, Loughborough, LE12 5RD, UK
[4] Laboratory of Parasitic Diseases, College of Veterinary Medicine, Shanxi Agricultural University, Taigu, Shanxi Province 030801, PR China
[5] Key Laboratory of Veterinary Public Health of Higher Education of Yunnan Province, College of Veterinary Medicine, Yunnan Agricultural University, Kunming, PR China

Contact information for the corresponding author:
Prof Xing-Quan Zhu
Email: xingquanzhu1@hotmail.com
Tel: +86-18793138037

Abstract

Several calcium-binding proteins including calcium-dependent protein kinases, play important roles in several facets of the intracellular infection cycle of the apicomplexan protozoan parasite *Toxoplasma gondii*. However, the role of the calcium binding epidermal growth factor (EGF) domain-containing proteins (CBDPs) remains poorly understood. In this study, we examined the functions of four *CBDP* genes in *T. gondii* RH strain of Type I by generating knock-out strains using CRISPR-Cas9 system. We investigated the ability of mutant strains deficient in *CBDP1*, *CBDP2*, *CBDP3* or *CBDP4* to form plaques, replicate intracellularly, and egress the host cells. The results showed that no definite differences between any of these four *CBDP* mutant strains and the wild-type strain in terms of their ability to form plaques, intracellular replication, and egress. Additionally, *CBDP* mutants did not exhibit any significant attenuated virulence compared to the wild-type strain in mice. The expression profiles of *CBDP2-4* genes were conserved among *T. gondii* strains of different genotypes, life cycle stages, and developmental forms. Whether other *CBDP* genes play any roles in the pathogenicity of *T. gondii* strains of different genotypes remains to be elucidated.

Keywords: *Toxoplasma gondii* · Calcium binding EGF domain-containing protein (CBDP) · CRISPR-Cas9 system · Gene functions

Introduction

The globally prevalent protozoan *Toxoplasma gondii* can infect humans and a large number of avian and mammalian species (Elsheikha et al. 2021; Robert-Gangneux and Dardé 2012; Smith et al. 2021). *T. gondii* infection occurs via ingestion of raw or poorly cooked meat containing the parasite tissue cysts or drinking water contaminated with oocysts excreted in the feline feces (Wang et al. 2019). *T. gondii* infection in immunocompetent individuals rarely causes any clinical symptoms. However, this parasite can lead to life-threatening conditions in patients with a compromised immune system, such as those with AIDS or malignancies (Elsheikha et al. 2021; Wang et al. 2017). *T. gondii* can also be transmitted vertically via the placenta to the fetus, which can lead to miscarriage, premature birth, fetal malformation, or stillbirth (Elsheikha, 2008; Robert-Gangneux and Dardé 2012; Rico-Torres et al. 2016; Smith et al. 2021).

Ca^{2+} is a signalling molecule involved in a wide range of cellular processes in eukaryotic mammalian cells and regulates the host cell invasion, parasite motility, and egress in *T. gondii* (Borges-Pereira et al. 2015; Lovett and Sibley 2003; Lourido et al. 2013; Nagamune et al. 2008). Calcium storage organelles in *T. gondii* are located in the Golgi, endoplasmic reticulum (ER), mitochondria, apicoplast, and a plant-like vacuole (Moreno and Docampo 2003; Moreno et al. 2011; Pingret et al. 1996). Calcium-binding proteins (CBP) include calmodulin (CAM), calmodulin neuropilin B-like proteins (CBL), and calcium-dependent protein kinases (CDPK), all have highly conserved EF-chiral structural domains (Moreno et al. 2011). At least twelve CDPKs (CDPK1, CDPK2, CDPK2A, CDPK2B, CDPK3, CDPK4, CDPK4A, CDPK5, CDPK6, CDPK7, CDPK8 and CDPK9) are expressed in *T. gondii* (Billker et al. 2009), and several CDPKs are involved in the parasites propagation. For example, *CDPK1* plays a role in the motility, host-cell invasion and egress of *T. gondii* (Lourido et al. 2010), while deletion of

CDPK2 causes the accumulation of starch granules in the bradyzoite stage, leading to morphological defects and inhibition of cyst formation (Uboldi et al. 2015; Wang et al. 2018). CDPK3 plays important roles in parasite egress and cyst formation in the brain of mice (Garrison et al. 2012; Kannan et al. 2021; Wu et al. 2022). Downregulation of *CDPK7* causes division and growth defects in *T. gondii* (Morlon-Guyot et al. 2014). On the other hand, *CDPK4*, *CDPK4A*, *CDPK5*, *CDPK6*, *CDPK8* and *CDPK9* are non-essential genes and are not involved in the invasion, egress and intracellular proliferation or virulence of *T. gondii* (Long et al. 2016; Wang et al. 2015). In calmodulin (CaM)-like proteins, calcium binds and regulates the functions of many different partner proteins, including motor proteins, ion channels, and other enzymes (Kursula et al. 2014). A large number of CaM proteins have been identified in *T. gondii* including a single highly conserved CaM gene, and numerous CaM-like genes (Nagamune and Sibley 2006). CaM1 and CaM2 are individually dispensable, but the loss of both genes results in a lethal phenotype, whereas CaM3 is refractory to deletion. All three genes (CaM1, CaM2 and CaM3) contribute to parasite motility, host cell invasion, and egress (Long et al. 2017).

Epidermal growth factor (EGF) is a short peptide with a distinctive motif of six cysteines which is found in many proteins and performs various functions (Davis et al. 1990). EGF or EGF-like domains have been reported in many membrane-bound proteins (Appella et al. 1988; Blomquist et al. 1984; Barker et al. 1986; Doolittle et al. 1984; Davis et al. 1990). In *T. gondii*, TgMIC3 is a microneme protein containing five overlapping EGF-like domains (Garcia-Reguet et al. 2000), which assists parasite attachment and invasion (Zhang et al. 2019). A calcium-binding site has been found at the N terminus of some EGF-like domains (Selander-Sunnerhagen et al. 1992). Apicomplexan parasites, such as *T. gondii*, rely on calcium as a signalling molecule to regulate various cellular processes (Lourido et al. 2013). Calcium-binding may be crucial for protein-protein interactions and potentially parasite protein-host

interactions. However, knowledge of the role of the calcium binding EGF domain-containing proteins (CBDPs) in the replication and infectivity of *T. gondii* is limited.

Identification of the genes required for the infectivity of *T. gondii* is essential for understanding the parasite intracellular replication cycle as well as development of effective anti-*T. gondii* strategies. Although numerous parasite genes important for *T. gondii* pathogenicity have been identified, it is likely that additional genes remain to be discovered. In the present study, we sought to uncover the role *T. gondii* CBDPs in the replication and virulence of *T. gondii* Type I RH strain. We investigated whether the deletion of *CBDP1*, *CBDP2*, *CBDP3* and *CBDP4* using the CRISPR-Cas9 gene editing technology affects the parasite plaque formation, intracellular replication, and egress. The impact of *CBDP* gene deletion on the parasite virulence and acute *T. gondii* infection in mice was also investigated.

Materials and methods

Mice and parasites

Female Kunming mice of 7–8 weeks old were purchased from the Centre of Laboratory Animals, Lanzhou Veterinary Research Institute, Chinese Academy of Agricultural Sciences. All mice were raised under specific pathogen-free and biocontainment conditions with free access to water and food as well as environmental enrichment. The tachyzoites of *T. gondii* RH strain (Type I) and the corresponding knockout strains were cultured in human foreskin fibroblasts (HFFs, American Type Culture Collection, Manassas, VA, USA) maintained at 37 °C in a 5% CO_2 air atmosphere, as previously described (Wang et al. 2020b).

Generation of *CBDP* knockout strains by CRISPR-Cas9 system

The CRISPR/Cas9 target selection website (http://www.e-crisp.org/E-CRISP/) was used for prediction of the four target genes (*TGGT1_315520*, *TGGT1_318540*, *TGGT1_269930* and

TGGT1_315550) of *T. gondii* RH strain. The details of the primers used are listed in Table 1. The pSAG1::CAS9-U6::sgUPRT was used as a template and the UPRT targeting guide RNA was replaced with the corresponding guide RNAs using the Q5 fixed-point mutagenesis kit (NEB). The primers listed in Table 2 were used to amplify the 3′ and 5′ homologous arms of each *CBDP* gene from the genomic DNA of *T. gondii* RH strain. The plasmid pUPRT-DHFR-D was used as a template to amplify the DHFR fragment. The 5′ and 3′ homologous sequences of each gene were obtained by amplification of the genomic DNA of the RH strain, and the DHFR fragment was amplified from the pUPRT-DHFR-D plasmid. The above sequences were inserted into the PUC19 vector using a multi-fragment cloning method using the Clone Express II one-step Cloning Kit (Vazyme). After transformation, positive plasmids were identified by sequencing and the positive plasmid was extracted using Endo-Free Plasmid DNA Mini Kit Protocols (OMEGA). Finally, the corresponding gene specific CRISPR plasmid (30 μg) and the homology construct (25 μg) were co-transfected into freshly egressed tachyzoites ($n=10^7$), and the positive strains were screened by 3 μM pyrimethamine. Finally, 96-well plates were used to isolate single clones and *T. gondii* DNA was extracted and verified by PCR using previously designed primers (Table 3) (Wang et al. 2020a).

Assessment of the plaque formation

We examined the ability of the mutant and wild-type strains to produce plaques in HFF tissue culture. Briefly, HFF monolayers in 12-well culture plates were infected with 500 freshly egressed tachyzoites per well. After 7 days of incubation at 37°C, the infected cell cultures were washed gently with phosphate buffered saline (PBS) three times. After fixation with 4% paraformaldehyde (PFA) for 10 min, the infected monolayers were stained for 15 min with 0.2% crystal violet to visualize the plaques. The stained monolayers were imaged using a scanner to

analyse the relative size and number of plaques formed by the growing tachyzoites, as previously described (Wang et al. 2020a).

Intracellular replication of tachyzoites

We investigated the effect of *CBDP* gene deletion on the intracellular replication of *T. gondii*. In brief, HFF monolayers grown on 12-well culture plates were infected with 10^5 freshly egressed tachyzoites per well for 1 h, and then washed with PBS to remove unbound tachyzoites. The plates were incubated for further 23 h and then the cell monolayers were fixed with 4% PFA and tachyzoites were stained with anti-SAG1. At least 200 parasitophorous vacuoles (PVs) were examined using the microscope to determine the number of tachyzoites (1, 2, 4, 8, and 16 tachyzoites) within each PV. The percentage of the PVs containing different numbers of tachyzoite was calculated as previously described (Garrison et al. 2012; Shen and Sibley 2014).

Egress assay

HFF monolayers growing in 12-well tissue culture plates were infected with 2×10^4 tachyzoites of each of the deletion strains and the wild-type RH strain. After 30-36 h of incubation, the infected cells were treated with 3 μM calcium ionophore A23187 1:1000 in Dulbecco's Modified Eagle Medium and tachyzoites egress from host cells was recorded immediately by time-lapse microscopic imaging as previously described (McCoy et al. 2012; Morlon-Guyot et al. 2014).

Mouse infection with the mutant strains

Kunming mice were infected with 100 freshly egressed tachyzoites of each of the four *CBDP* knockouts or the wild-type strains (6 mice/strain) by intraperitoneal (i.p.) injection. All mice

were monitored and weighed daily for any clinical signs, and twice daily if they started to show a change in their appetite, body weight, behavior, level of activity, or posture. Mice were euthanized immediately on reaching the humane endpoint.

Bioinformatic analysis of *T. gondii* calcium binding EGF domain-containing proteins

The CBDP proteins were analyzed for the presence of functional domains using the SMART tool as previously described (Zhang et al. 2020). Information on the genomic characteristics (such as signal peptide, the number of exons and transmembrane domains) and time-series expression data of the *CBDP* genes were obtained from the ToxoDB (Gajria et al. 2007). Data was representative to *T. gondii* cell cycle phases, life cycle stages (oocyst, tachyzoite and bradyzoite), and genotypes (I, II and III). We compared the cell cycle stages of the RH strain for *CBDP2* (*TGGT1_318540*), *CBDP3* (*TGGT1_269930*) and *CBDP4* (*TGGT1_315550*) as previously described (Behnke et al. 2010).

Statistical analysis

All statistical analyses were performed using GraphPad Prism 9 (GraphPad Software, La Jolla, CA, USA) and the level of significance was determined by one-way ANOVA or two-way ANOVA as indicated in the figure legends. Survival differences were tested for statistical significance by the log rank (Mantel-Cox) test. Each experiment was repeated three times, and the results were shown as means ± standard deviations (SD), and the difference was considered significant when the p-value was < 0.05.

Results

Identification of the functional domains of CBDPs

The prediction of the functional domains of the amino acid sequences of *TGGT1_315520*, *TGGT1_318540*, *TGGT1_269930* and *TGGT1_315550* of *T. gondii* RH strain was performed by using the SMART tool. We detected the presence of EGF, epidermal growth factor calcium-binding (EGF-CA) and EGF-like domains, showing that these proteins are CBDPs (Fig. S1).

Successful construction and validation of the *CBDP* knockout strains

To investigate the functions of the four TgCBDPs, the CRISPR-Cas9 technique was used to delete the *CBDP* genes, individually, in Type I RH strain, and the CBDP coding region was successfully replaced by 5′ UTR-DHFR-3′ UTR fragment using a homologous recombination system (Fig. 1A). Single clones were obtained by drug selection and limiting dilution assay. The primers in Table 3 were used to validate the construction of mutant strains. As shown in Fig. 1B, in the four mutant strains (RHΔ*CBDP1*, RHΔ*CBDP2* RHΔ*CBDP3* and RHΔ*CBDP4*), the PCR2 targeting ~600 bp *CBDP* fragment did not produce any amplicons, confirming the absence of the targeted gene in the knocked-out strain. Additionally, replacement of DHFR fragment was confirmed by PCR1 and PCR3, with ~1500 bp fragment being amplified in the KO strains but was not detected in the wild-type RH strain (Fig. 1B), indicating the successful construction of four *CBDP* deletion mutant strains.

Deletion of *CBDP1-4* does not affect the parasite ability to form plaques

To explore the potential involvement of *CBDP1-4* in the parasite infectivity, we began by testing the effect of deleting *CBDP1-4* on the ability of *T. gondii* to form plaques in cultured cells. There was no significant difference in the number or the size of the plaques between any of the four knockout strains and the corresponding wild-type RH strain ($p > 0.05$, Fig. 2A-B). This result suggests that *CBDP1-4* play no roles in *T. gondii* replication.

CBDP1-4 are not involved in the egress and replication of *T. gondii*

As the plaque assay is limited by the parasite's ability to cause cell lysis and plaque formation in the host cell monolayer, it does not discern the changes that occur at the different stages of the lytic infection cycle. Therefore, it was important to investigate additional properties of the mutant strains such as the egress process and the intracellular replication kinetics. The results showed that the majority of tachyzoites of the four *CBDP* mutant strains and the wild-type strain egressed from host cells within 2 min, without any significant differences between all the examined strains (Fig. 3A). We also tested the extent to which the deletion of *CBDP1-4* affects the intracellular growth dynamics of tachyzoites inside the PVs. We found that largest proportion of the vacuoles contained 16 tachyzoites. However, the numbers of tachyzoites inside the PVs were not significantly different between any of the four deletion strains and the wild-type RH strain ($p > 0.05$, Fig. 3B).

CBDP1-4 do not mediate the virulence of *T. gondii* in mice

To gain insight into the role of *CBDP1-4* in the parasite virulence, we inoculated five groups of Kunming mice (6 mice/ group) with 100 tachyzoites of each deletion mutant strain or the wild-type RH strain by i.p. injection. The results showed that all 5 groups of mice reached their humane endpoint between 9 and 12 dpi. The survival time of mice inoculated with each of the four deletion strains was slightly prolonged compared with mice infected by the wild-type strain, however the difference was not significant ($p > 0.05$, Fig. 4).

Sequence characteristics and expression patterns of *CBDP*s in *T. gondii*

Table 4 summarizes the bioinformatic characteristics of the four *CBDP* genes. We found that none of the four *CBDP* genes had signal peptides. The *CBDP1*, *CBDP3* and *CBDP4* had transmembrane regions, but *CBDP2* did not. Most of the *CBDP* genes were encoded by multiple

exons, with *CBDP3* having the largest number. To corroborate the results from the *in vitro* and *in vivo* studies, we analyzed the expression levels of the four genes in different genotypes of *T. gondii* strains, parasite cell cycles, and different life-cycle stages. The *CBDP1* (*TGGT1_315520*) did not have any representative transcriptome in the ToxoDB and therefore *CBDP1* was not included in the bioinformatic analysis. The expression profiles of the three *CBDP2-4* genes did not follow a specific cell cycle pattern, with a higher expression of *CBDP3* and a lower expression for *CBDP2* and *CBDP4* (Fig. S2A). Next, we analysed the transcript levels of the 3 *CBDP* genes in different genotypes of *T. gondii* (Type I, Type II and Type III) (Fig. S2B) and found that *CBDP3* of RH strain (genotype I) had a slightly higher expression, compared with the expression levels of *CBDP2* and *CBDP4* of the same strain. However, for Type II and Type III, the expression levels of the three genes were similar. Our analysis revealed that all three *CBDP* genes were differentially expressed at different life cycle stages, with *CBDP4* being significantly higher than *CBDP2* and *CBDP3* in oocysts sporulated for 4 days; the expression of the three *CBDP* genes was lower after 2 days *in vitro* (Fig. S2C).

Discussion

The present study was undertaken to identify the role of *CBDP* genes in the pathogenicity and infection process of *T. gondii.* The study did not detect any significant differences in the intracellular replication between the four *CBDP* mutant strains and the wild-type RH strain. Likewise, no significant differences were detected in the parasite egress between the mutant and wild-type strains. Additionally, no significant differences were observed between the wild-type RH strain and any of the four CBDP mutant strains in regard to the number or size of plaques, which is a direct reflection of the extent of infection-related cell monolayer damage, and thus, is used as a proxy of *T. gondii* virulence (Liang et al. 2021). These results suggest that the four *CBDP* genes are not essential for *T. gondii* growth, replication, or pathogenicity.

We also examined the possibility that these four *CBDP* genes are involved in the parasite virulence. Our *in vivo* data showed that all 5 groups of Kunming mice, infected by RHΔ*CBDP1*, RHΔ*CBDP2*, RHΔ*CBDP3* and RHΔ*CBDP4* or wild-type RH strain, have reached their humane endpoint between 9-12 days. There was no significant difference in the survival rate between mice infected by *CBDP*-mutant-type and those infected by wild-type RH strain. Whether the deletion of *CBDPs* can influence the cyst formation in the mouse brain remains to be investigated.

T. gondii has a complex life cycle and its development involves alternations between biologically distinct stages, which involves significant transcriptional changes (Chen et al. 2018; Radke et al. 2010; Sharma et al. 2020). Likewise, the pathogenic effect of this obligate intracellular parasite requires direct engagement with the host cell in numerous lytic cycles involving cell invasion, intracellular replication and egress, culminating in the destruction of the host cell. The transition between these distinct steps of *T. gondii* lytic cycle is accompanied by marked changes in gene expression (Gaji et al. 2011; Lescault et al. 2010). Furthermore, significant differences were detected in the proteome (Zhou et al. 2017), phosphoproteome (Wang et al. 2019) and post-translational modification (Nie et al. 2022) between *T. gondii* strains of different genetic and virulence backgrounds.

In the present study, we characterized the transcriptomic expression levels of *CBDP2-4* genes. Our bioinformatic analysis revealed low expression of *CBDP2-4* in *T. gondii* strains of Types I, II and III, with *CBDP3* of RH strain (genotype I) having a slightly higher expression, compared with the expression levels of *CBDP2* and *CBDP4* of the same strain. Additionally, there were low expression levels and non-significant differences between different phases of the parasite lytic cycle and the different life cycle forms obtained *in vitro* or *in vivo*. These results suggest that the expression profiles of *CBDP* genes were conserved between the different lytic cycle phases, genotypes, and life cycle forms of *T. gondii*. Given the remarkable

transcriptomic changes that underpin the parasite alternation between different stages and phases during its developmental cycle (Chen et al. 2018; Fritz et al. 2012; Radke et al. 2005; Sharma et al. 2020) and infection cycle (Gaji et al. 2011; Lescault et al. 2010), the lack of definite differences in the expression patterns of *CBDP2-4* genes across lytic cycle phases, genotypes, life cycle forms is consistent with the non-essential role of *CBDP2-4* genes in the replication and virulence of *T. gondii* RH strain.

Conclusion

Here, we examined the biological roles of *CBDP1*, *CBDP2*, *CBDP3* and *CBDP4* in the pathogenicity of *T. gondii* RH strain *in vitro* and *in vivo*. CRISPR-Case9-mediated disruption of the four *CBDP* genes showed that none of these genes is essential for the parasite virulence or lytic cycle including intracellular replication, plaque formation, and egress. These results were consistent with the high CRISPR fitness and limited transcriptional changes of these genes between the parasite cell cycle phases, genotypes and life cycle forms. Further investigations are required to elucidate the specific roles of other *CBDP* genes in the establishment and maintenance of *T. gondii* infection.

Acknowledgments We thank Professor Bang Shen, Huazhong Agricultural University for providing the pSAG1-Cas9-SgUPRT and pUPRT-DHFR-D vectors.

Declarations

Funding

Project support was provided by the National Natural Science Foundation of China (Grant No. 32002306), Fundamental Research Funds of the Chinese Academy of Agricultural Sciences

(Grant No. 1610032021017), the Fund for Shanxi “1331 Project” (Grant No. 20211331-13), The Agricultural Science and Technology Innovation Program (ASTIP) of China (Grant No. CAAS-ASTIP-2016-LVRI-03), the Yunnan Expert Workstation (Grant No. 202005AF150041) and the Veterinary Public Health Innovation Team of Yunnan Province (Grant No. 202105AE160014).

Conflicts of interest

The authors declare that they have no competing interests.

Availability of data and material

The datasets supporting the findings of this article are included within the paper and its supplementary materials.

Authors’ contributions

Xing-Quan Zhu, Meng Wang, Jin-Lei Wang and Hany M. Elsheikha conceived and designed the study. Xin-Cheng Wang performed the experiments, analysed the data and wrote the manuscript. Ting-Ting Li, Xiao-Nan Zheng and Dan-Yu Zhao participated in the implementation of the study. Meng Wang and Jin-Lei Wang contributed reagents/materials/analysis tools. Hany M. Elsheikha, Xing-Quan Zhu and Meng Wang critically revised the manuscript. All authors read and approved the final version of the manuscript.

Ethics approval

All animal studies were carried out in accordance with protocols reviewed and approved by the Research Ethics Committee of Lanzhou Veterinary Research Institute, Chinese Academy of Agricultural Sciences. All animals were handled strictly according to the Animal Ethics

Procedures and Guidelines of the People's Republic of China. All efforts were made to minimize the number of mice used in the study.

Consent to participate

Not applicable.

Consent for publication

Not applicable.

Supplementary Information

The online version contains supplementary material available at: xxxx

References

Appella E, Weber IT, Blasi F (1988) Structure and function of epidermal growth factor-like regions in proteins. FEBS Lett 231(1):1-4

Behnke MS, Wootton JC, Lehmann MM, Radke JB, Lucas O, Nawas J, Sibley LD, White MW (2010) Coordinated progression through two subtranscriptomes underlies the tachyzoite cycle of *Toxoplasma gondii*. PLoS One 5:e12354

Billker O, Lourido S, Sibley LD (2009) Calcium-dependent signaling and kinases in apicomplexan parasites. Cell Host Microbe 5(6):612-622

370 Blomquist MC, Hunt LT, Barker WC (1984) Vaccinia virus 19-kilodalton protein: relationship
371 to several mammalian proteins, including two growth factors. Proc Natl Acad Sci U S A
372 81(23):7363–7367
373 Borges-Pereira L, Budu A, McKnight CA, Moore CA, Vella SA, Hortua Triana MA, et al.
374 (2015) Calcium signaling throughout the *Toxoplasma gondii* lytic cycle: A Study using
375 genetically encoded calcium indicators. J Biol Chem 290(45):26914-26926
376 Chen LF, Han XL, Li FX, Yao YY, Fang JP, Liu XJ, Li XC, Wu K, Liu M, Chen XG (2018)
377 Comparative studies of *Toxoplasma gondii* transcriptomes: insights into stage conversion
378 based on gene expression profiling and alternative splicing. Parasit. Vectors 11, 402
379 Davis CG (1990) The many faces of epidermal growth factor repeats. New Biol 2(5):410–419
380 Doolittle RF, Feng DF, Johnson MS (1984) Computer-based characterization of epidermal
381 growth factor precursor. Nature 307(5951):558–560
382 Elsheikha HM (2008) Congenital toxoplasmosis: priorities for further health promotion action.
383 Public Health 122(4):335-353
384 Elsheikha HM, Marra CM, Zhu XQ (2021) Epidemiology, pathophysiology, diagnosis, and
385 management of cerebral toxoplasmosis. Clin Microbiol Rev 34(1):00115-19
386 Fritz HM, Buchholz KR, Chen X, Durbin-Johnson B, Rocke DM, Conrad PA, Boothroyd JC
387 (2012) Transcriptomic analysis of *Toxoplasma* development reveals many novel functions
388 and structures specific to sporozoites and oocysts. PloS one 7(2):e29998
389 Gaji RY, Behnke MS, Lehmann MM, White MW, Carruthers VB (2011) Cell cycle-dependent,
390 intercellular transmission of *Toxoplasma gondii* is accompanied by marked changes in
391 parasite gene expression. Mol Microbiol 79:192–204

392 Gajria B, Bahl A, Brestelli J, Dommer J, Fischer S, Gao X, Heiges M, Iodice J, Kissinger J,
393 Mackey A, Pinney D, Roos D, Stoeckert C, Wang HM, Brunk B (2007) ToxoDB: an
394 integrated *Toxoplasma gondii* database resource. Nucleic Acids Res 36(Database
395 issue):D553-556
396 Garcia-Réguet N, Lebrun M, Fourmaux MN, Mercereau-Puijalon O, Mann T, Beckers CJ,
397 Samyn B, Van Beeumen J, Bout D, Dubremetz JF (2000) The microneme protein MIC3
398 of *Toxoplasma gondii* is a secretory adhesin that binds to both the surface of the host cells
399 and the surface of the parasite. Cell Microbiol 2(4):353-364
400 Garrison E, Treeck M, Ehret E, Butz H, Garbuz T, Oswald B, Settles M, Boothroyd J,
401 Arrizabalaga G (2012) A forward genetic screen reveals that calcium-dependent protein
402 kinase 3 regulates egress in *Toxoplasma*. PLoS Pathog 8(11):e1003049
403 Kannan G, Thaprawat P, Schultz TL, Carruthers VB (2021) Acquisition of host cytosolic
404 protein by *Toxoplasma gondii* bradyzoites. mSphere 6(1):e00934-20
405 Kursula P (2014) The many structural faces of calmodulin: a multitasking molecular jackknife.
406 Amino acids 46(10):2295–2304
407 Lescault PJ, Thompson AB, Patil V, Lirussi D, Burton A, Margarit J, Bond J, Matrajt M (2010)
408 Genomic data reveal *Toxoplasma gondii* differentiation mutants are also impaired with
409 respect to switching into a novel extracellular tachyzoite state. PLoS ONE 5:e14463
410 Liang QL, Nie LB, Li T. T., Elsheikha HM, Sun LX, Zhang ZW, Zhao D.Y, Zhu X.Q, Wang
411 JL (2021) Functional characterization of 17 protein serine/threonine phosphatases in
412 *Toxoplasma gondii* using CRISPR-Cas9 system. Front Cell Dev Biol 9(10):738794

413 Long S, Wang Q, Sibley LD (2016) Analysis of noncanonical calcium-dependent protein
414 kinases in *Toxoplasma gondii* by targeted gene deletion using CRISPR/Cas9. Infect
415 Immun 84(5):1262-1273
416 Long S, Brown KM, Drewry LL, Anthony B, Phan IQH, Sibley LD (2017) Calmodulin-like
417 proteins localized to the conoid regulate motility and cell invasion by *Toxoplasma gondii*.
418 PLoS Pathog 13(5):e1006379
419 Lourido S, Jeschke GR, Turk BE, Sibley LD (2013) Exploiting the unique ATP-binding pocket
420 of *Toxoplasma* calcium-dependent protein kinase 1 to identify its substrates. ACS Chem
421 Biol 8(6):1155-1162
422 Lourido S, Shuman J, Zhang C, Shokat KM, Hui R, Sibley L. D (2010) Calcium-dependent
423 protein kinase 1 is an essential regulator of exocytosis in *Toxoplasma*. Nature
424 465(7296):359-362
425 Lovett JL, Sibley LD (2003) Intracellular calcium stores in *Toxoplasma gondii* govern invasion
426 of host cells. J Cell Sci 116(Pt 14):3009-3016
427 McCoy JM, Whitehead L, van Dooren GG, Tonkin CJ (2012) TgCDPK3 regulates calcium-
428 dependent egress of *Toxoplasma gondii* from host cells. PLoS Pathog 8(12):e1003066
429 Moreno SNJ, Docampo R (2003) Calcium regulation in protozoan parasites. Curr Opin
430 Microbiol 6(4):359-364
431 Moreno SNJ, Ayong L, Pace DA (2011) Calcium storage and function in apicomplexan
432 parasites. Essays Biochem 51:97-110

433 Morlon-Guyot J, Berry L, Chen CT, Gubbels MJ, Lebrun M, Daher W (2014) The *Toxoplasma*
434 *gondii* calcium-dependent protein kinase 7 is involved in early steps of parasite division
435 and is crucial for parasite survival. Cell Microbiol 16(1):95-114
436 Nagamune K, Sibley LD (2006) Comparative genomic and phylogenetic analyses of calcium
437 ATPases and calcium-regulated proteins in the apicomplexa. Mol Biol Evol 23(8):1613–
438 1627
439 Nagamune K, Moreno SN, Chini EN, Sibley LD (2008) Calcium regulation and signaling in
440 apicomplexan parasites. Subcell Biochem 47:70-81
441 Nie LB, Liang QL, Wang M, Du R, Zhang MY, Elsheikha HM, Zhu XQ (2022) Global profiling
442 of protein lysine malonylation in *Toxoplasma gondii* strains of different virulence and
443 genetic backgrounds. PLoS Negl Trop Dis 16(5):e0010431
444 Pingret L, Millot JM, Sharonov S, Bonhomme A, Manfait M, Pinon JM (1996) Relationship
445 between intracellular free calcium concentrations and the intracellular development of
446 *Toxoplasma gondii*. J Histochem Cytochem 44(10):1123-1129
447 Radke JB, Lucas O, Nawas J, Sibley LD, White MW (2010) Coordinated progression through
448 two subtranscriptomes underlies the tachyzoite cycle of *Toxoplasma gondii*. PloS one
449 5(8):e12354
450 Radke JR, Behnke MS, Mackey AJ, Radke JB, Roos DS, White MW (2005) The transcriptome
451 of *Toxoplasma gondii*. BMC Biol 3:26
452 Rico-Torres CP, Vargas-Villavicencio JA, Correa D (2016) Is *Toxoplasma gondii* type related
453 to clinical outcome in human congenital infection? systematic and critical review. Eur J
454 Clin Microbiol Infect Dis 35(7):1079-1088

455 Robert-Gangneux F, Dardé ML (2012) Epidemiology of and diagnostic strategies for
456 toxoplasmosis. Clin Microbiol Rev 25(2):264-296
457 Selander-Sunnerhagen M, Ullner M, Persson E, Teleman O, Stenflo J, Drakenberg T (1992)
458 How an epidermal growth factor (EGF)-like domain binds calcium. High resolution NMR
459 structure of the calcium form of the NH2-terminal EGF-like domain in coagulation factor
460 X. J Biol Chem 267(27):19642-19649
461 Sharma J, Rodriguez P, Roy P, Guiton PS (2020) Transcriptional ups and downs: patterns of
462 gene expression in the life cycle of *Toxoplasma gondii*. Microbes Infect. 22(10):525-533
463 Shen B, Sibley LD (2014) *Toxoplasma* aldolase is required for metabolism but dispensable for
464 host-cell invasion. Proc Natl Acad Sci U S A 111(9):3567-3572
465 Smith NS, Goulart C, Hayward JA, Kupz A, Miller CM, van Dooren GG (2021) Control of
466 human toxoplasmosis. Int J Parasitol 51(2-3):95-121
467 Uboldi AD, McCoy JM, Blume M, Gerlic M, Ferguson DJP, Dagley LF, Beahan CT, Stapleton
468 DI, Gooley PR, Bacic A, Masters SL, Webb AI, McConville MJ, Tonkin CJ (2015)
469 Regulation of starch stores by a Ca^{2+}-dependent protein kinase is essential for viable cyst
470 development in *Toxoplasma gondii*. Cell Host Microbe 18(6):670-681
471 Wang JL, Bai MJ, Elsheikha HM, Liang QL, Li TT, Cao XZ, Zhu XQ (2020a) Novel roles of
472 dense granule protein 12 (GRA12) in *Toxoplasma gondii* infection. FASEB J 34(2):3165-
473 3178
474 Wang JL, Li TT, Elsheikha HM, Chen K, Cong W, Yang WB, Bai MJ, Huang SY, Zhu XQ
475 (2018) Live attenuated Pru:Δcdpk2 strain of *Toxoplasma gondii* protects against acute,
476 chronic, and congenital toxoplasmosis. J Infect Dis 218(5):768-777

Wang JL, Liang QL, Li TT, He JJ, Bai MJ, Cao XZ, Elsheikha HM, Zhu XQ (2020b) *Toxoplasma gondii* tkl1 deletion mutant is a promising vaccine against acute, chronic, and congenital toxoplasmosis in mice. J Immunol 204(6):1562-1570

Wang JL, Zhang NZ, Li TT, He JJ, Elsheikha HM, Zhu XQ (2019) Advances in the development of anti-*Toxoplasma gondii* vaccines: challenges, opportunities, and perspectives. Trends Parasitol 35(3):239-253

Wang S, Hassan IA, Liu X, Xu L, Yan R, Song X, Li X (2015) Immunological changes induced by *Toxoplasma gondii* glutathione-S-transferase (TgGST) delivered as a DNA vaccine. Res Vet Sci 99:157-164

Wang ZD, Wang C, Liu HH, Ma HY, Li ZY, Wei F, Zhu XQ, Liu Q (2017) Prevalence and burden of *Toxoplasma gondii* infection in HIV-infected people: a systematic review and meta-analysis. Lancet HIV 4(4):e177-e188

Wang ZX, Zhou CX, Calderón-Mantilla G, Petsalaki E, He JJ, Song HY, Elsheikha HM, Zhu XQ (2019) iTRAQ-based global phosphoproteomics reveals novel molecular differences between *Toxoplasma gondii* strains of different genotypes. Front Cell Infect Microbiol. 29:307

Wu, M., An, R., Zhou, N., Chen, Y., Cai, H., Yan, Q., Wang, R., Luo, Q., Yu, L., Chen, L., & Du, J (2022) *Toxoplasma gondii* CDPK3 controls the intracellular proliferation of parasites in macrophages. Front Immunol 13:905142

Zhang D, Jiang N, Chen Q (2019) ROP9, MIC3, and SAG2 are heparin-binding proteins in *Toxoplasma gondii* and involved in host cell attachment and invasion. Acta Trop 192:22-29

Zhang H, Liu J, Ying Z, Li S, Wu Y, Liu Q (2020) *Toxoplasma gondii* UBL-UBA shuttle proteins contribute to the degradation of ubiquitinylated proteins and are important for synchronous cell division and virulence. FASEB J 34(10):13711-13725

Zhou DH, Wang ZX, Zhou CX, He S, Elsheikha HM, Zhu XQ (2017) Comparative proteomic analysis of virulent and avirulent strains of *Toxoplasma gondii* reveals strain-specific patterns. Oncotarget 8(46):80481-80491

507 **Table 1** Construction of the *CBDP* knockout *T. gondii* RH strains.

Primer name	Sequence (5' → 3')
Sg-315520	GCGGCGATTATCGAGAGCTAGTTTTAGAGCTAGAAATAGC
Sg-318540	GATCATCTCCTCTAACAAGTGTTTTAGAGCTAGAAATAGC
Sg-269930	GAAGACAACGAACCAGGCCAGTTTTAGAGCTAGAAATAGC
Sg-315550	GGTTATACGGAGACCAGCGCGTTTTAGAGCTAGAAATAGC

508 Note: The underlined sequence is the sgRNA.

509

510

511

512

513 **Table 2** Primers for amplification of homologous fragments.

Primer name	Sequence (5' → 3')
U5-315520-F	GGTTTTCCCAGTCACGACGTTTCTGGGAGGAAGGACACGAGCAA
U5-315520-R	GGATTTACAGCCTGGCGAAGCTTTTTCAACCCCTGAGCGAAAAGC
U3-315520-F	CTATGCACTTGCAGGATGAATTCTATGCTTCGGTCTTTTATGTTCCTGG
U3-315520-R	GAGCGGATAACAATTTCACAACGCCAACTGGTCGGGTGATT
U5-318540-F	GGTTTTCCCAGTCACGACGTTAGCCTCTTGCGGAGTCTTGTGG
U5-318540-R	GGATTTACAGCCTGGCGAAGCTTGTATGCTGGCACCGACGGAGAT
U3-318540-F	CTATGCACTTGCAGGATGAATTCGGAAGTGGCTGCTGGCGTTTT
U3-318540-R	GAGCGGATAACAATTTCACACATCGGTTCGTAATTCATTGTTATTGTCT
U5-269930-F	GGTTTTCCCAGTCACGACGTTTGTTTGGAGGGAGGCTAGAAGTGC
U5-269930-R	GGATTTACAGCCTGGCGAAGCTTACGATAGAAGACGCCGAAATGGTTA
U3-269930-F	CTATGCACTTGCAGGATGAATTCTTCAGCAACATCGTTCCACCCC
U3-269930-R	GAGCGGATAACAATTTCACAATATTTCTTGTCCAGAAACCGGATTACAT
U5-315550-F	GGTTTTCCCAGTCACGACGTTGCTGCTGCTTGGCTTCCCTCA
U5-315550-R	GGATTTACAGCCTGGCGAAGCTTTGTCCTTTCGGTTGAAAATGTCGC
U3-315550-F	CTATGCACTTGCAGGATGAATTCCAAGGTTGTGCGGGGCAGGTC
U3-315550-R	GAGCGGATAACAATTTCACATGGCTTCGATGGTTGTCTTTCCAG

514 Note: The underlined sequences are designed to amplify homologous fragments.
515
516
517
518
519
520
521
522
523
524
525
526
527
528

529 **Table 3** Primers used for the confirmation of the targeted gene deletion.

Primer name	Sequence (5' → 3')
315520-PCR1-F	GGGAAGGAAATGCACGGTGGATTA
315520-PCR2-F	CCACTTAGATGGGACGGGATTGC
315520-PCR2-R	TGAGTGAGACAGTGCTTCCACCAGA
315520-PCR3-R	CTCCGACTTTCCGAGATTTCGCTT
318540-PCR1-F	TTCTGCCCCTTCACAACCACAGTT
318540-PCR2-F	CGGAGGATTTGAATGCGGTTGC
318540-PCR2-R	CCCGATGTTAGTTTTGGTGATGTTTG
318540-PCR3-R	GCCGAGTGCGATAAGAGTGATTGT
269930-PCR1-F	CGCATGAGAACGTTGGTTCACCTG
269930-PCR2-F	GTCTTAGGATTTGATGCTTGTCTGATGG
269930-PCR2-R	GAAGTGAAAAGTAACAGGAGCTGGGTC
269930-PCR3-R	GTTTGCGCACAGAAACTGGCATGT
315550-PCR1-F	CCCAGCAGTTGATCGATCTCGATA
315550-PCR2-F	CAACGGATTTTCGTCTAATGAGGTCTT
315550-PCR2-R	CCATCGGACTCCTGGCTGACC
315550-PCR3-R	AAGGTTCTGTTCTGCCTCTTCCGA
PCR1-R	GCCAAAGTAGAAAGGAATTAGCAT
PCR3-F	TGACGCAGATGTGCGTGTATCCAC

530
531
532

Table 4 Bioinformatics features of the CBDPs of *Toxoplasma gondii*.

Name	Gene ID	Product description	Exons	Phenotype value	TMHMM[a]	Molecular weight (kD[a])	Predicted signal peptide
CBDP1	TGME49_315520	Calcium binding egf domain-containing protein	8	1.04	Yes	36.589	No
CBDP2	TGME49_318540	Calcium binding egf domain-containing protein	2	0.77	No	72.334	No
CBDP3	TGME49_269930	Calcium binding egf domain-containing protein	13	-0.14	Yes	337.852	No
CBDP4	TGME49_315550	Calcium binding egf domain-containing protein	7	0.85	Yes	33.195	No

Note: [a] Prediction of transmembrane helices was carried out using the TMHMM, program version 2.0.

Figures:

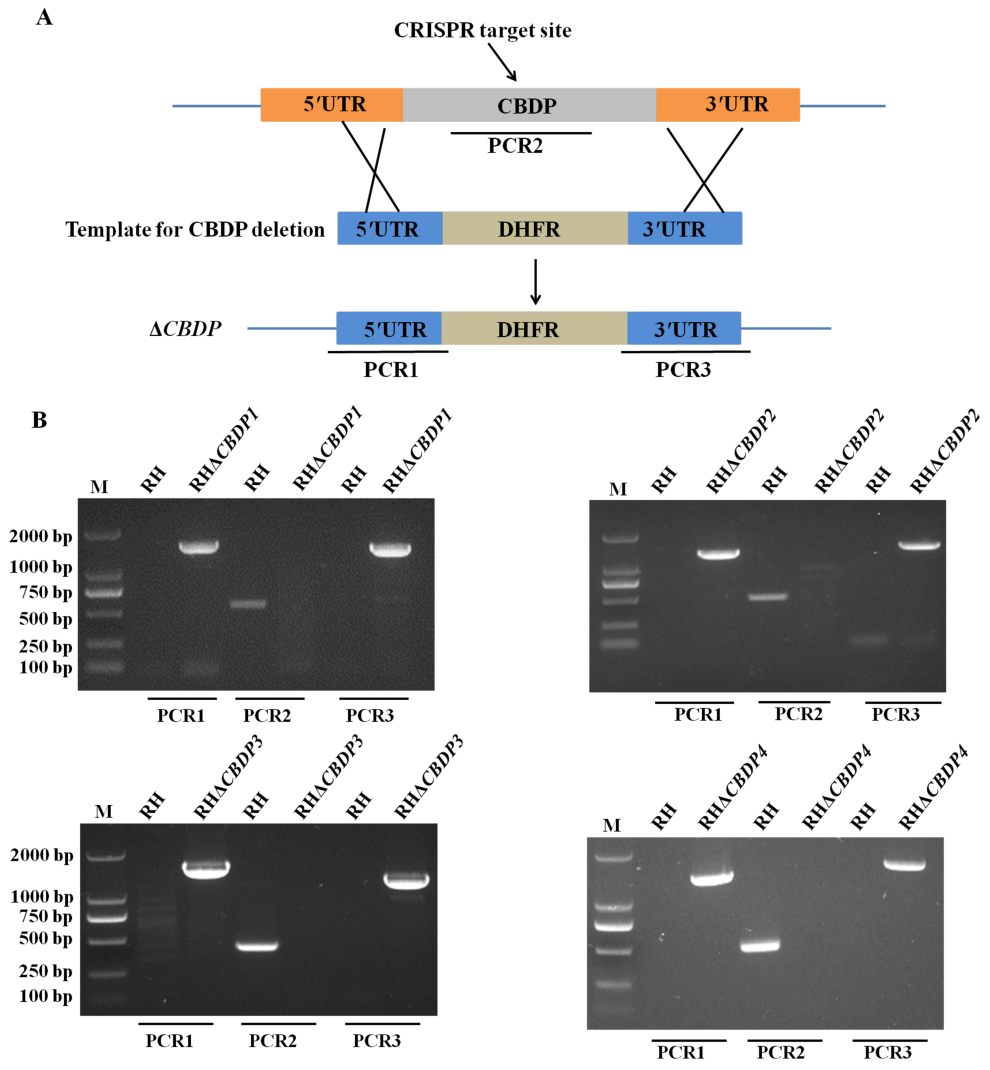

Fig. 1 Construction of the *CBDP* knockout strains using CRISPR-cas9 technology. **A** Schematic diagram showing the disruption of the targeted *CBDP* genes. **B** The knockout strains (RHΔ*CBDP1*, RHΔ*CBDP2*, RHΔ*CBDP3* and RHΔ*CBDP4*) were verified by PCR analysis. PCR1 and PCR3 amplified ~ 1500 bp band in knockout strains, while wild-type RH strain had no band, indicating that DHFR fragments were successfully inserted into knockout strains from 5' to 3' ends by homologous recombination. PCR2 showed that ~ 600 bp band was amplified in the wild-type RH strain, while knockout strains had no bands, showing that the targeted genes were successfully deleted.

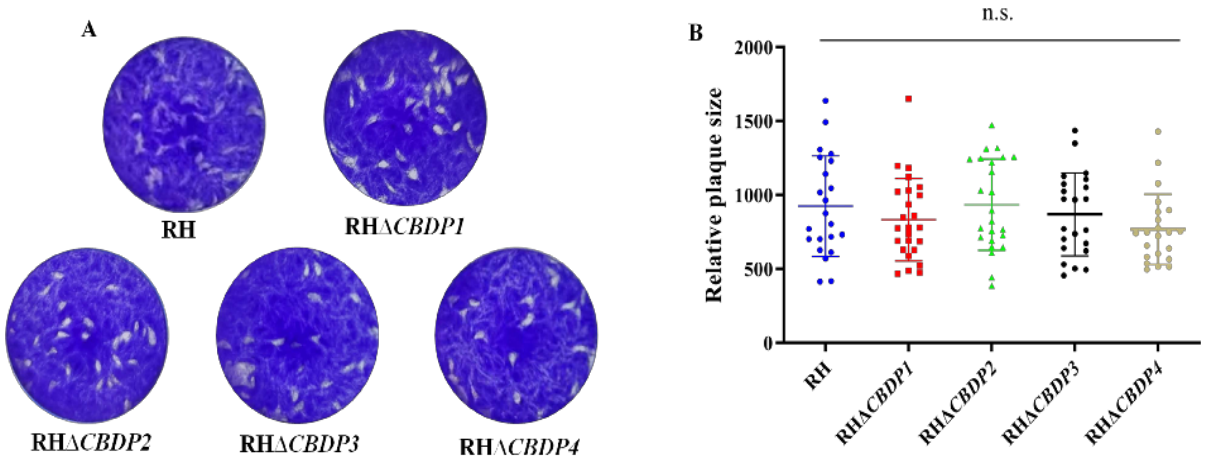

Fig. 2 The plaque formation of *CBDP* knockout strains compared with wild-type RH strain *in vitro*. HFF monolayers were infected by 500 tachyzoites for 7 days and stained with crystal violet to determine the number of plaques. **A** Representative photographs of the plaques detected in HFFs infected by the 4 RHΔ*CBDP1-4* strains and those produced by the wild-type RH strain. **B** The relative size of the plaques generated by *CBDP1-4* mutant strains versus the wild-type RH strain showing no significant differences between RH strain and any *CBDP* mutant strains. n.s, not significant, one-way ANOVA.

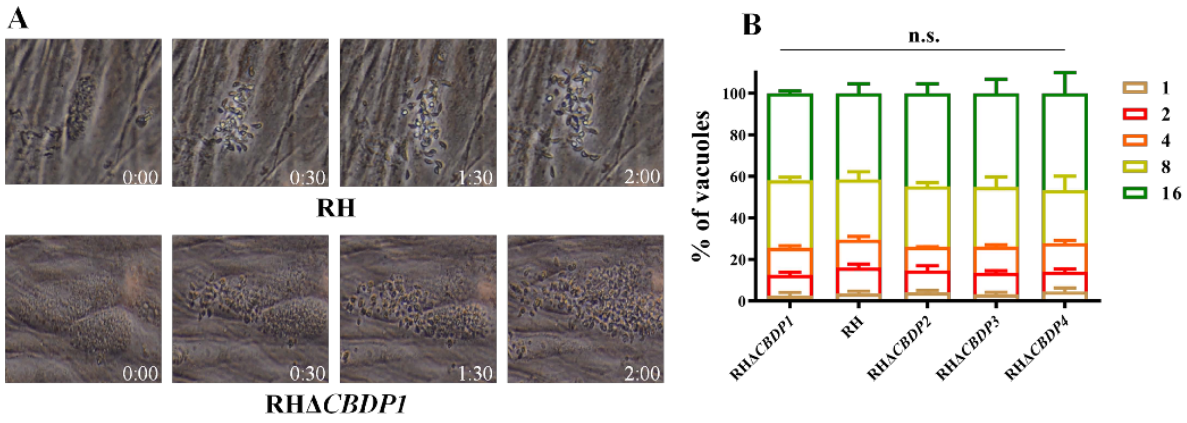

Fig. 3 Egress process and intravacuolar replication of the *CBDP* knockout strains and wild-type RH strains *in vitro*. After inoculation of 2×10^4 tachyzoites of the CBDP mutant and wild type RH strains into HFF monolayers grown in 12 plates for 28-32 h, the culture medium was discarded. The tachyzoite exist of the host cells was recorded after adding 3 μM of calcium ionophore A23187. **A** Representative images showing that one of the *CBDP1-4* mutant strains (RHΔ*CBDP1*) and the wild-type RH strain egress during 2 min after adding 3 μM calcium ionophore A23187. **B** The percentages of the parasitophorous vacuoles containing tachyzoites (1, 2, 4, 8, and 16 tachyzoites per vacuole). The wild-type RH strain and the *CBDP1-4* mutant strains had roughly similar intracellular replication dynamics. n.s., not significant, two-way ANOVA.

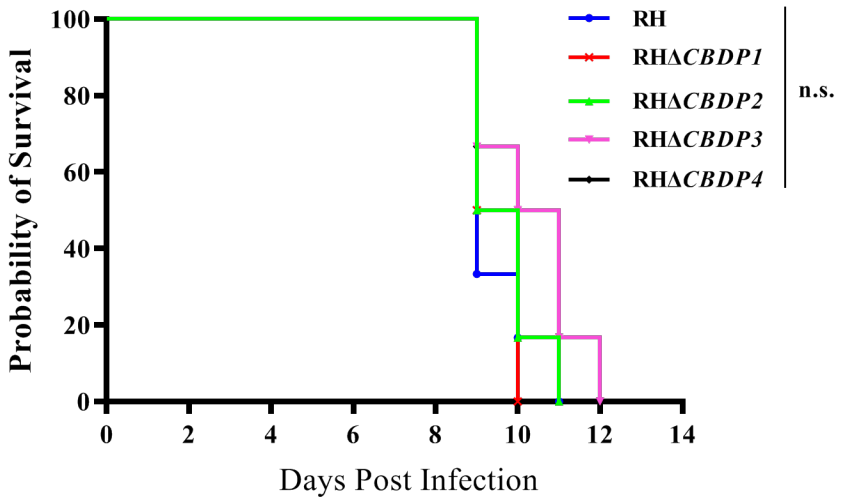

Fig. 4 Survival curve of the Kunming mice infected by the *CBDP* mutant strains and wild-type RH strain of *T. gondii*. The mice (6/group) were intraperitoneally injected with 100 tachyzoites of each strain. Following infection, the mice reached their humane endpoint within 9 to 12 days after infection. Statistical analysis was performed with GraphPad Prism. Log-rank (Mantel-Cox) tests and revealed no statistically significant differences (p >0.05)

Supplementary information

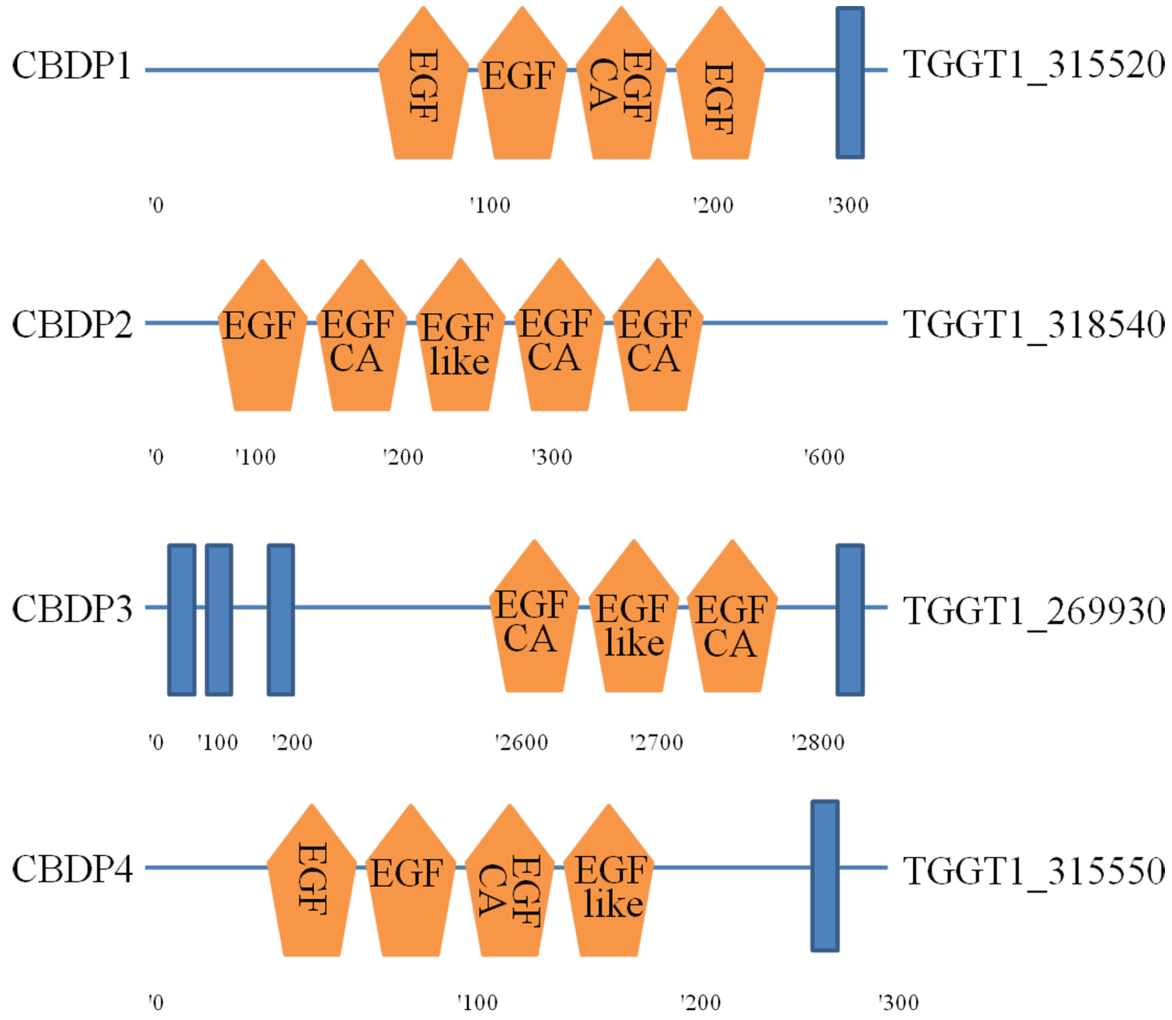

Fig. S1 The schematic diagram of the predicted functional domains in each CBDP protein. EGF, epidermal growth factor-like domain; EGF-CA, calcium- binding EGF-like domain; EGF-like, EGF domain, unclassified subfamily. The putative functional domains of the CBDP proteins were predicated by the SMART algorithm (http://smart.embl-heidelberg.de). The blue rectangles represent the transmembrane helix region, as detected by the TMHMM v2.0 program.

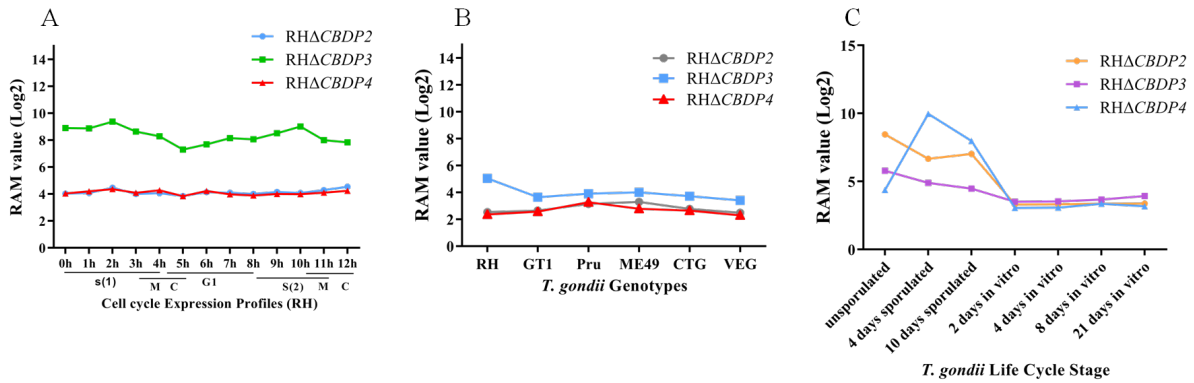

621

622 **Fig. S2** The expression profiles of *Toxoplasma gondii CBDP*s. **A** The expression profile of 3
623 *CBDP* genes of *T. gondii* RH strain presented by the cell cycle phases. **B** The expression profiles
624 of 3 *CBDP* genes in Type I (RH and GT1), Type II (Pru and ME49), and Type III (CTG and
625 VEG) strains. **C** The expression profiles of 3 *CBDP* genes related to the parasite life cycle
626 stages (oocyst, tachyzoite and bradyzoite). Expression profile of 3 *CBDP* genes of the oocysts
627 recovered from cat feces at 0 day (unsporulated), 4 days (4 days sporulated), and 10 days (10
628 days sporulated), tachyzoites grown for 2 days in HFF cells (2 days *in vitro*), bradyzoites grown
629 in HFF cells for 4 days and 8 days (4 day *in vitro* and 8 days *in vitro*), and 21 days tissue cyst-
630 containing bradyzoites harvested from infected mouse brains (21 days *in vivo*). Each line
631 represents the expression value of the corresponding gene.

632